Q. J. R. Meteorol. Soc. (2001), **127**, pp. 1183–1197

Surface fluxes under shear-free convection

By E. AKYLAS[1], M. TOMBROU[1]*, D. LALAS[2] and S. S. ZILITINKEVICH[3]

[1] *University of Athens, Greece*
[2] *National Observatory of Athens, Greece*
[3] *Uppsala University, Sweden*

(Received 24 February 2000; revised 17 October 2000)

SUMMARY

In this study, theoretical models of Schumann, Sykes *et al.*, Beljaars, and Zilitinkevich *et al.* are examined, compared with data, and evaluated with regard to the calculation of the minimum friction velocity and the heat transfer coefficient. All data employed in earlier papers, namely those from meteorological campaigns SCOPE, TOGA COARE and BOREX-95, and the Schmidt and Schumann and Sykes and Henn large-eddy simulations (LESs), are considered. To achieve objective comparison between different formulae, empirical coefficients are recalculated by fitting theoretical curves separately for field data and for data from LESs. Despite essential differences in the shapes of the vertical profiles and the surface-layer height formulations applied in different models, practically all of them perform rather similarly and in fairly good correspondence with the chosen data set. However, a remarkable systematic difference is observed between data from measurements, on the one hand, and LES data, on the other. It is argued that this difference results from a contribution from uncounted mean-wind shear to the friction velocity in the field experiments. By this expedient, applicability of LESs to the resistance and heat–mass transfer problem is confirmed, and empirical coefficients in the resistance and heat transfer formulations are refined.

KEYWORDS: Heat fluxes Large-eddy simulation Minimum friction velocity Monin–Obukhov Surface layer

1. INTRODUCTION

The traditional Monin–Obukhov (M–O) similarity theory breaks down in the case of shear-free convection. Indeed, in calm weather, the M–O theory predicts no friction in the surface layer, and consequently a low level of mixing at the very surface. During the last decade, however, it has been recognized that convective boundary layers (CBLs) are affected by large eddies. These eddies produce essential convergence/divergence flow patterns in the surface layer even in the absence of a mean wind (Businger *et al.* 1971; Businger 1973; Schumann 1988; Sykes *et al.* 1993; Beljaars 1995; Zilitinkevich *et al.* 1998). The velocity-scale inherent in these large eddies is the Deardorff (1970, 1972) convective velocity-scale,

$$W_* = (B_S h)^{1/3}. \tag{1}$$

Here, h is the height of the inversion, which acts as a lid to the convective flow, and B_S the buoyancy flux at the surface, which is related to the surface heat flux, Q_S, by,

$$B_S = \frac{g}{\theta} Q_S, \tag{2}$$

where g is the acceleration due to gravity, and θ is the potential temperature.

Clearly, the surface-layer scaling should be extended to include the Deardorff velocity-scale, W_*, and consequently the CBL depth, h.

Businger (1973) was the first to propose the idea of extra shear in the convective surface layer, due to large eddies, regardless of the possible absence of a mean wind. He introduced the concept of the 'minimum friction velocity' U_* (the square root of the absolute value of the variable surface shear due to large eddies in calm weather) and the

* Corresponding author: Laboratory of Meteorology, Department of Physics, University of Athens, Panepistimioupolis, Build. Physics V, Athens 15784, Greece.

'convective surface-layer length.'

$$L_* = \frac{U_*^3}{k_u B_s} = \frac{U_*^3 h}{k_u W_*^3}, \tag{3}$$

where k_u is the von Kármán constant for velocity ($\approx$0.4).

He also proposed that the surface friction and the heat transfer depend on the CBL governing parameters, Q_s and h, and the surface roughness through universal unknown functions,

$$\begin{aligned} \frac{U_*}{W_*} &= f_1\left(\frac{h}{z_{0u}}\right), \\ \frac{Q_s}{\Delta\theta W_*} &= f_2\left(\frac{h}{z_{0u}}, \frac{z_{0T}}{z_{0u}}\right), \end{aligned} \tag{4}$$

where $\Delta\theta$ is the temperature difference across the surface layer, and $z_{0\{u,T\}}$ are the roughness lengths for momentum and temperature, respectively (for the difference between these two see Brutsaert (1982) and Garratt (1992)). The functions f_1 and f_2 are expected to be monotonically decreasing. The form of functions f_1 and f_2 has been a subject of much investigation by Schumann (1988), Sykes *et al.* (1993), Beljaars (1995), and Zilitinkevich *et al.* (1998). They proposed different theoretical formulations, where the coefficients were estimated by fitting to available data. Schmidt and Schumann (1989), Sykes *et al.* (1993) and Beljaars (1995) used data from large-eddy simulations (LES)s. Zilitinkevich *et al.* (1998) utilized data from field measurements TOGA COARE* (Fairall *et al.* 1996), SCOPE† (Kropfli and Clifford 1994) and BOREX-95‡ (Mikkelsen *et al.* 1996). They chose to rely only upon field data on turbulent fluxes, reasoning that they are obtained by direct measurements, whereas the near-surface fluxes in LESs are parametrized rather than directly simulated. They reckoned that LESs underestimate the fluxes, probably due to an inaccurate parametrization. In the present paper it is shown that the systematic positive difference between the field and the LES data on the fluxes is more naturally explained at the cost of the contribution from the mean-wind shear to the near-surface mixing. Indeed, the LESs in question simulated the genuine shear-free convection, which is practically never observed in nature. As a result, field data are always affected by some shear.

The functions f_1 and f_2, Eq. (4), are intended for parametrization of the surface fluxes in practically oriented numerical models, where the best combination between accuracy and simplicity is demanded. Therefore, it is important to compare different formulations and to identify their advantages and disadvantages. Grachev *et al.* (1997) compared some earlier formulations for f_1 employing data from measurements over the sea (TOGA COARE and SCOPE campaigns) related to very low values of z_{0u}.

In the present paper, a more comprehensive comparison is performed. It includes all basic schemes for f_1 and f_2 and expands the analysis to rough surfaces employing all available data, in particular data from measurements over land (BOREX-95) and earlier data from LESs.

* Tropical Ocean–Global Atmosphere Coupled Ocean–Atmosphere Response Experiment programme.
† San Clemente Ocean Probing Experiment.
‡ Borris Experiment, 1995.

2. SHORT DESCRIPTION OF THEORETICAL MODELS

The traditional M–O theory formulation, for the vertical gradients of the mean wind speed and potential temperature, employs the friction velocity, u_*, as a basic velocity-scale, the temperature scale, $-Q_S/u_*$, and the M–O length-scale, L. Roughly speaking, an advanced theory of the shear-free convection is nothing but an extension of the above theory through replacing u_* by the minimum friction velocity U_*, and L by the convective surface-layer length L_*, Eq. (3).

The common feature of the models examined here is the idea that the horizontal wind velocity, u, produced by the convective flow patterns, has its maximum at a reference height h_S, which is generally assumed to be the top of the surface layer. The scalar wind speed $u(h_S)$ is scaled by the Deardorff velocity, W_*, Eq. (1),

$$u(h_S) = C_u W_* \tag{5}$$

where C_u is a dimensionless empirical parameter.

Assuming that an M–O style treatment is now applicable up to the height $z = h_S$, the resistance and heat transfer coefficients become

$$\frac{U_*}{W_*} = C_u k_u \left\{ \ln\left(\frac{h_S}{z_{0u}}\right) - \Psi_u\left(\frac{h_S}{L_*}\right) + \Psi_u\left(\frac{z_{0u}}{L_*}\right) \right\}^{-1} \tag{6a}$$

$$\frac{Q_S}{\Delta\theta W_*} = \frac{k_T U_*}{W_*} \left\{ \ln\left(\frac{h_S}{z_{0T}}\right) - \Psi_T\left(\frac{h_S}{L_*}\right) + \Psi_T\left(\frac{z_{0T}}{L_*}\right) \right\}^{-1}. \tag{6b}$$

Here, k_T is the von Kármán constant for temperature ($\approx$0.4) and $\Psi_{\{u,T\}}$ are the unknown similarity functions. Equations of this type serve as a common basis for all the models considered in this work. Differences between models concern the specification of the wind-maximum height, h_S, and the shape of profiles in the height interval $0 < z < h_S$.

Schumann (1988) estimated the surface-layer height as $h_S = 0.1h$ (with reference to experimental evidence from Caughey (1982)), ignored the terms $\Psi_{\{u,T\}}(z_{0\{u,T\}}/L_*)$ on the right-hand side of Eq. (6) and substituted (for the sake of simplicity) z_{0u} for z_{0T}.

His most restrictive assumption was the exclusion of the logarithmic term from the temperature-profile formulation, and the extrapolation of a purely convective $\sim z^{-1/3}$ profile down to the surface (Monin and Yaglom 1971; Grachev *et al.* 1997).

Schumann eventually derived the resistance and heat transfer laws in the form

$$\frac{U_*}{W_*} = a_u \left(\frac{h}{z_{0u}}\right)^{-1/6} \tag{7a}$$

$$\frac{Q_S}{\Delta\theta W_*} = (4k_u k_T^3)^{1/3} \left(\frac{h}{z_{0u}}\right)^{-1/3} = \frac{(4k_u k_T^3)^{1/3}}{a_u^2} \left(\frac{U_*}{W_*}\right)^2. \tag{7b}$$

These equations do not include C_u. Later on Grachev *et al.* (1997) also employed a purely convective profile and derived a similar formulation.

Beljaars (1995) employed the Paulson (1970) approximation for $\Psi_{\{u,T\}}$ based on the Kansas-type function for unstable stratification (Businger *et al.* 1971). Using a modified version of the Paulson equations for very strong instability (very large values of $-h_S/L_*$), he eliminated h_S. Eventually he derived the desired relationships in the

form

$$\frac{U_*}{W_*} = C_u k_u \left\{ \ln\left(\frac{-38.5L_*}{16z_{0u}}\right) + \Psi_u\left(\frac{z_{0u}}{L_*}\right)\right\}^{-1} \tag{8a}$$

$$\frac{Q_s}{\Delta\theta W_*} = \frac{U_*}{W_*} k_T \left\{ \ln\left(\frac{-L_*}{4z_{0T}}\right) + \Psi_T\left(\frac{z_{0T}}{L_*}\right)\right\}^{-1}. \tag{8b}$$

Sykes *et al.* (1993) assumed that the stability effects on the vertical profiles are negligible (took $\Psi_{\{u,T\}} = 0$) and applied a simplified version of the horizontal momentum equation to obtain

$$\frac{h_s}{h} = a_1^{-1}\left(\frac{U_*}{W_*}\right)^2. \tag{9}$$

Then employing Eq. (9) and substituting z_{0u} for z_{0T}, the following relationships were obtained:

$$\ln\left(\frac{h}{z_{0u}}\right) = C_u k_u \frac{W_*}{U_*} + 2\ln\left(\frac{W_*}{U_*}\right) + \ln a_1 \tag{10a}$$

$$\frac{Q_s}{\Delta\theta W_*} = \frac{1}{C_u a_T k_u}\left(\frac{U_*}{W_*}\right)^2. \tag{10b}$$

The dimensionless parameters, in the above formulations, were estimated by their authors using data from LESs.

Zilitinkevich *et al.* (1998) developed a more detailed model, considering typical convergence flow patterns as internal boundary layers affected by the buoyancy forces. Accordingly, they assumed that the logarithmic profiles change into the power-law profiles (of the type $z^{-1/3}$) at the matching height $z = C_* L_*$ (where $C_* \sim 0.1$), which in turn gradually change shape as the wind maximum height, $z = h_s$, is approached. Then the vertical gradients of the horizontal velocity and potential temperature became

$$\frac{\partial u}{\partial z} = \begin{cases} \dfrac{U_*}{k_u z} & \text{at } z \leqslant C_* L_* \\ \dfrac{C_U U_*^2}{B_s^{1/3} z^{4/3}}\left\{1 - \left(\dfrac{z}{h_s}\right)^{4/3} f_u\left(\dfrac{z}{h_s}\right)\right\} & \text{at } C_* L_* \leqslant z \leqslant h_s \end{cases} \tag{11a}$$

$$\frac{\partial \theta}{\partial z} = \begin{cases} -\dfrac{Q_s}{k_T U_* z} & \text{at } z \leqslant C_* L_* \\ -\dfrac{C_T Q_s}{B_s^{1/3} z^{4/3}}\left\{1 - \left(\dfrac{z}{h_s}\right)^{4/3} f_T\left(\dfrac{z}{h_s}\right)\right\} & \text{at } C_* L_* \leqslant z \leqslant h_s. \end{cases} \tag{11b}$$

Here, $f_{\{u,T\}}(z/h_s)$ are unknown functions reflecting the effect of the internal boundary layer on the shape of the profiles, and C_U and C_T are dimensionless parameters. Furthermore, Zilitinkevich *et al.* (1998) estimated h_s as the area-averaged height of the internal boundary layer, which gave $h_s = ah$. Finally, integrating Eqs. (11) over z from

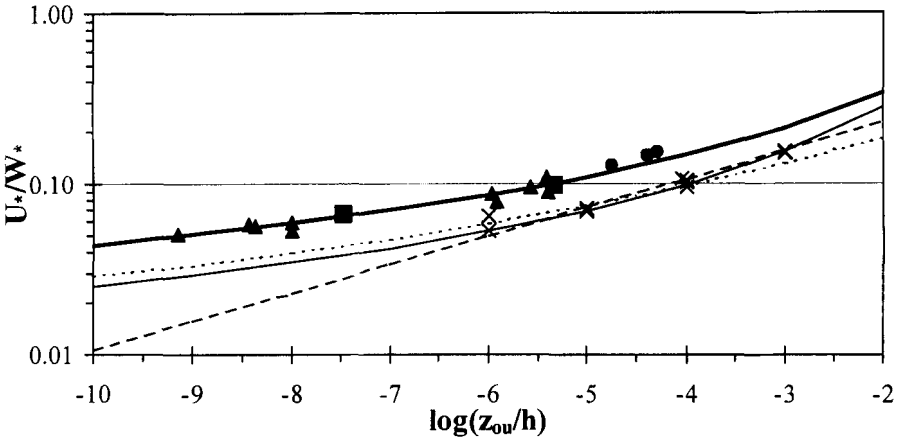

Figure 1. The dimensionless minimum friction velocity, U_*/W_*, versus the ratio of the roughness length to the convective boundary layer depth, z_{0u}/h. Empirical coefficients in theoretical models are from the original studies: in the Schumann (dashed line), Sykes *et al.* (thin line) and Beljaars (dotted line) models—calculated by fitting to large-eddy simulation data (×), and in the Zilitinkevich *et al.* model (heavy line), by fitting to TOGA COARE (▲), SCOPE (■) and BOREX-95 (•) field data, see text.

0 to h_s they derived the resistance and heat transfer laws in the form

$$\ln\left(\frac{h}{z_{0u}}\right) = c_{u0}k_u\frac{W_*}{U_*} + 3\ln\left(\frac{W_*}{U_*}\right) - c_{u1} + c_{u2}\left(\frac{W_*}{U_*}\right)^{-1} \tag{12a}$$

$$C_{AH}^{-1} \equiv \frac{\Delta\theta U_*}{Q_s} - k_T^{-1}\ln\left(\frac{z_{0u}}{z_{0T}}\right) = c_{T0}\frac{W_*}{U_*} - c_{T1} + c_{T2}\left(\frac{W_*}{U_*}\right)^{-1}. \tag{12b}$$

Here, dimensionless empirical parameters c_{u0}, c_{u1}, c_{u2}, c_{T0}, c_{T1}, c_{T2} depend on a, C_u, C_U and C_T through the relations

$$\left.\begin{aligned} C_{u0} &= C_u k_u & c_{T0} &= \frac{c_{u0}}{k_T} \\ c_{u1} &= \frac{3k_u^{4/3}C_U}{C_*^{1/3}} + \ln\frac{C_*}{k_u} & c_{T1} &= \frac{c_{u1}}{k_T} - \frac{3k_u^{1/3}C_T}{C_*^{1/3}} - \frac{\ln(C_*/k_T)}{k_T} \\ c_{u2} &= \frac{(3+A)k_u C_U}{a^{1/3}} & c_{T2} &= \frac{c_{u2}}{k_T} - \frac{(3+B)C_T}{a^{1/3}} \\ A &= \int_{C_*L_*/ah}^{1} f_u(\xi)\,\mathrm{d}(\xi) & B &= \int_{C_*L_*/ah}^{1} f_T(\xi)\,\mathrm{d}(\xi). \end{aligned}\right\} \tag{13}$$

The left-hand side of Eq. (12b) is the reciprocal of the aerodynamic heat transfer coefficient, C_{AH}, based on the minimum friction velocity, U_*. It is applied to exclude the difference between the roughness lengths for scalars and for momentum from the right-hand side of the equation. Given C_{AH} and z_{0T}, a useful and practical heat transfer coefficient, $Q_s/\Delta\theta W_*$, based on the Deardorff velocity-scale, W_*, is immediately obtained.

It is worth noticing that the Sykes *et al.* (1993) Eq. (10a) and the Zilitinkevich *et al.* (1998) Eq. (12a) are similar, except for the term $(W_*/U_*)^{-1}$ in Eq. (12a) reflecting the effect of the buoyancy forces on the wind profile.

TABLE 1. EMPIRICAL COEFFICIENTS IN THEORETICAL MODELS DEDUCED FROM LARGE-EDDY SIMULATION DATA BY THE MODEL AUTHORS AND IN THE PRESENT PAPER (BOLD)

Model	C_u	a_u	a_1	c_{u0}	c_{u1}	c_{u2}	a_T	c_{T0}	c_{T1}	c_{T2}
Schumann (1988)		0.5								
Sykes *et al.* (1993)	1.0		2.0				1.2			
Beljaars (1995)	1.2									
Zilitinkevich *et al.* (1998)	**0.9**			**0.4**	1.2	2.0		**0.8**	**3.1**	**4.0**
Eqs. (15) and (20)	**0.8**						**3.0**			

See text for definitions of coefficients.

TABLE 2. EMPIRICAL COEFFICIENTS IN THEORETICAL MODELS DEDUCED FROM FIELD DATA BY THE MODEL AUTHORS AND IN THE PRESENT PAPER (BOLD)

Model	C_u	a_u	a_1	c_{u0}	c_{u1}	c_{u2}	a_T	c_{T0}	c_{T1}	c_{T2}
Schumann (1988)		**0.8**								
Sykes *et al.* (1993)	**1.7**		**5.8**				**2.1**			
Beljaars (1995)	**1.8**									
Zilitinkevich *et al.* (1998)	1.7			0.6	1.2	2.0		1.5	1.7/**3.1**	2.0/**4.0**
Eqs. (15) and (20)	**1.6**						**3.0**			

See text for definitions of coefficients.

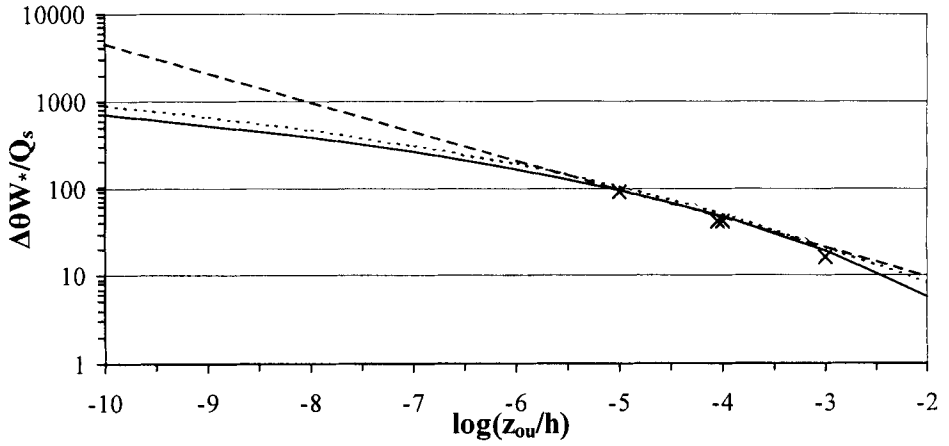

Figure 2. The reciprocal of the heat transfer coefficient, $\Delta\theta W_*/Q_S$, versus the ratio of the roughness length to the convective boundary-layer depth, z_{0u}/h. Empirical coefficients in the Schumann (dashed line), Sykes *et al.* (thin line) and Beljaars (dotted line) theoretical models are original, calculated by fitting to large-eddy simulation data (×). The roughness lengths z_{0T} and z_{0u} were taken as equal, see text.

In Fig. 1, the resistance-law formulations given by Eqs. (7a), (8a), (10a) and (12a) are shown together with data from field measurements (Kropfli and Clifford 1994; Fairall *et al.* 1996; Mikkelsen *et al.* 1996) and LESs (Schmidt and Schumann 1989; Sykes *et al.* 1993). All theoretical curves correspond to the original coefficients obtained by the model authors either from LESs (the first three models) or empirical data available at the time as in the Zilitinkevich *et al.* (1998) model (see Tables 1 and 2). A clear difference is observed between the earlier models and the Zilitinkevich *et al.* (1998) model, Eq. (12a), which predicts systematically higher values of U_*. It obviously deserves inquiring whether this difference is caused by the different physical nature of the models or whether it reflects the difference between experimental data and LESs.

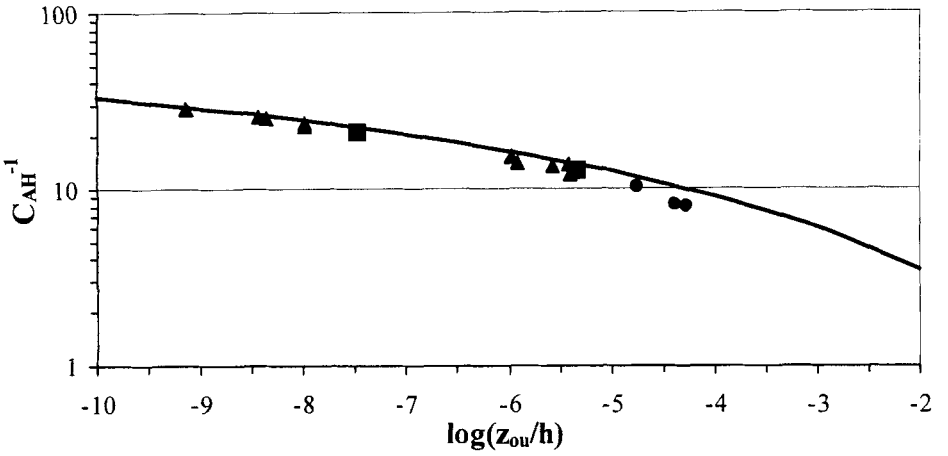

Figure 3. The reciprocal of the aerodynamic heat transfer coefficient, C_{AH}^{-1}, versus the ratio of the roughness length to the convective boundary-layer depth, z_{0u}/h. Empirical coefficients in the Zilitinkevich *et al.* theoretical model (heavy line) are original, calculated by fitting to TOGA COARE (▲), SCOPE (■) and BOREX-95 (●) field data.

As regards the heat transfer, the earlier models, Eqs. (7b), (8b) and (10b), presenting $Q_S/\Delta\theta W_*$ with empirical constants obtained from LESs, are shown in Fig. 2. The Zilitinkevich *et al.* Eq. (12b) presenting C_{AH} with empirical constants obtained from field data is shown in Fig. 3. For genuine comparison, all curves should be presented in the same format.

3. Recalculation of empirical parameters and evaluation of models

In the present paper, all empirical parameters are recalculated twice, using data from (i) LESs and (ii) field measurements. It is found that all schemes can be made more accurate through better specification of the coefficients. The schemes of Schumann (1988) and Sykes *et al.* (1993) are immediately extended to distinguish between z_{0u} and z_{0T}.

(*a*) *Resistance*

Modified curves representing the minimum friction velocity, U_*, with recalculated empirical coefficients based on either field measurements (Fig. 4) or LESs (Fig. 5) are very close to each other. Moreover, they all are in reasonable accordance with the data in question. Two alternative sets of empirical coefficients, field-data grounded and LES grounded, are given in Tables 1 and 2.

The Schumann (1988) Eq. (7a) based on field measurements (Fig. 4) agrees well with data at high values of the dimensionless roughness length ($z_{0u}/h > 10^{-6}$). However, at smaller values of z_{0u}/h it seriously underestimates U_*, which is caused by oversimplification of the profile (the extension of the $\sim z^{-1/3}$ profile down to the surface). Grachev *et al.* (1997) claimed that for strong convection over very rough surfaces, e.g. over a big city, the power law ($\sim z^{-1/3}$) dependence extends down to the surface, and the logarithmic portion in the profile no longer exists. This observation might help to illuminate why the Schumann model agrees well with field data for rough surfaces and with LES data, which all correspond to high values of z_{0u}/h.

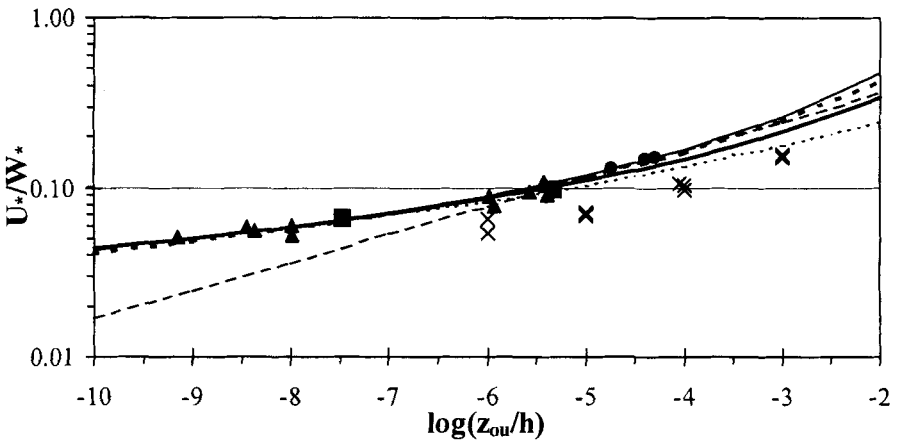

Figure 4. As in Fig. 1, but with all the empirical coefficients in the Schumann (dashed line), Sykes *et al.* (thin line), Beljaars (dotted line) and Zilitinkevich *et al.* (heavy line) calculated by fitting to the TOGA COARE (▲), SCOPE (■) and BOREX-95 (•) field data. Results from Eq. (15a) (heavy dotted line) are also illustrated. Large-eddy simulation data (×) are also presented for comparison.

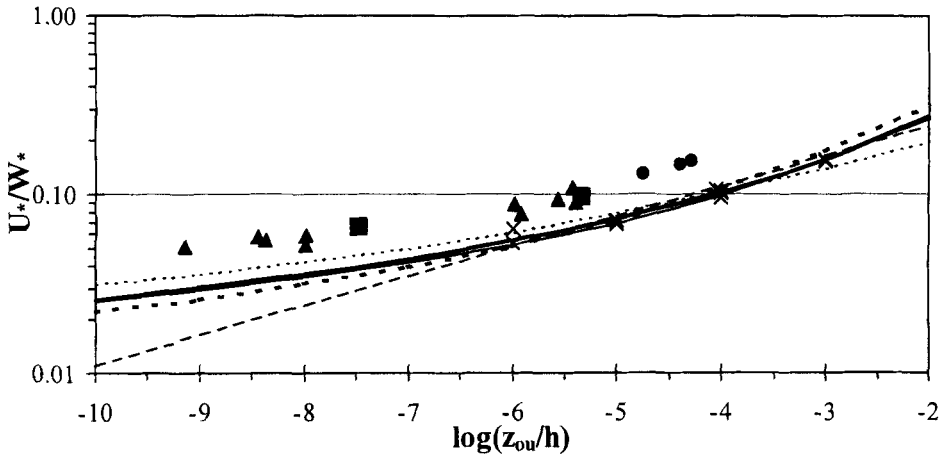

Figure 5. As in Fig. 4, but with all the empirical coefficients in the Schumann (dashed line), Sykes *et al.* (thin line), Beljaars (dotted line), Zilitinkevich *et al.* (heavy line) and Eq. (15a) (heavy dotted line) calculated by fitting to large-eddy simulation data (×). Field data for TOGA COARE (▲), SCOPE (■) and BOREX-95 (•) are also presented for comparison.

The Beljaars Eq. (8a) with the field-data grounded coefficients exhibits the opposite behaviour (Fig. 4). It agrees well with data at $z_{0u}/h < 10^{-5}$, but underestimates U_* at higher roughness lengths. This could be anticipated, since the Beljaars approximation of the Paulson function Ψ_u is justified only at very large values of $-z/L_*$. At the same time, even assuming that $h_s \sim h$, data from field measurements do not satisfy the above requirement at $z_{0u}/h > 10^{-5}$. It follows that over rough surfaces the wind profile has not enough room to level off (see discussion of Fig. 6 below). With the LES grounded coefficients (Fig. 5), the Beljaars approximation is more accurate due to the lower values of U_* and L_* (which causes levelling of the wind profile at $z = h_s$).

Using recalculated empirical coefficients, the Sykes *et al.* Eq. (10a) and the Zilitinkevich *et al.* Eq. (12a) show almost identical behaviour in the region $10^{-9} < z_{0u}/h <$

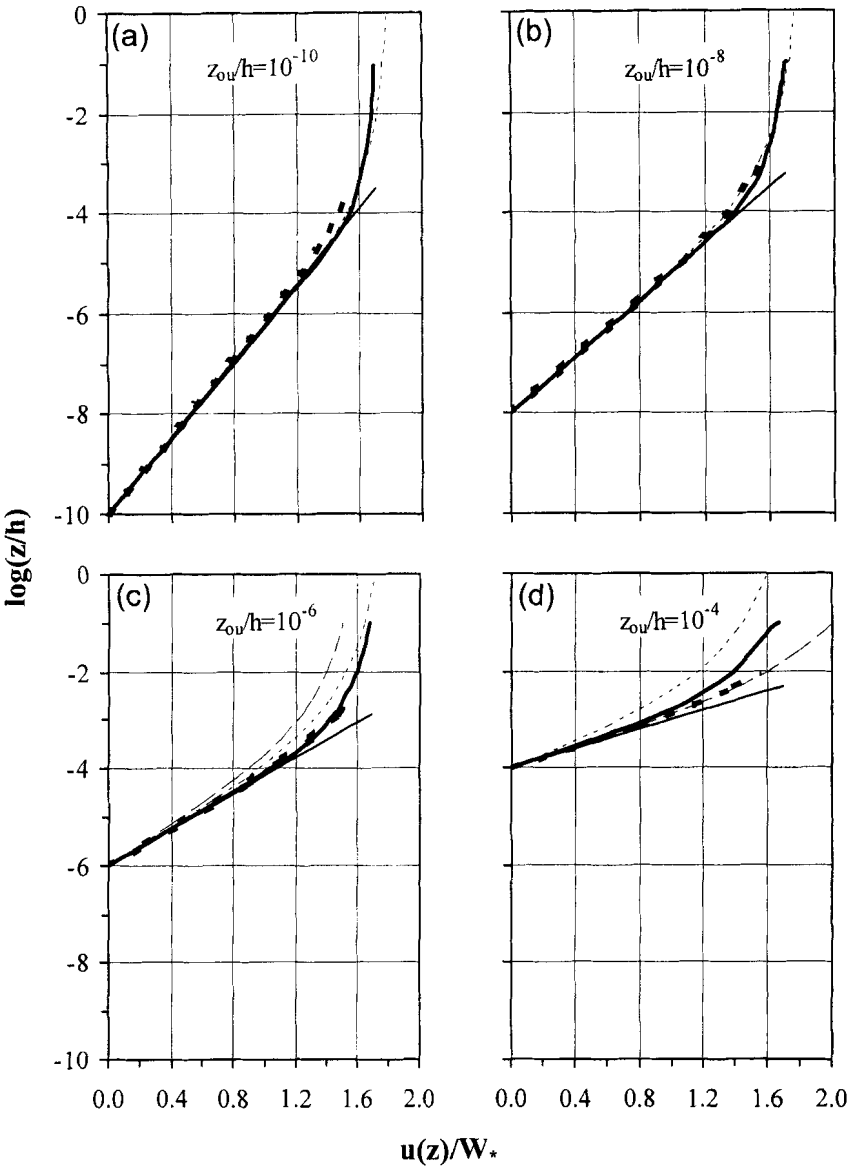

Figure 6. Dimensionless wind profiles, $u(z)/W_*$, versus the dimensionless height, z/h, applied in the models of Schumann (dashed lines), Sykes *et al.* (thin lines), Beljaars (dotted lines), Zilitinkevich *et al.* (heavy lines), and the present paper Eq. (15a) (heavy dotted lines). The profiles are plotted for different values of the dimensionless roughness length, z_{0u}/h: (a) 10^{-10}, (b) 10^{-8}, (c) 10^{-6} and (d) 10^{-4}.

10^{-5}, whereas at higher roughness lengths the Sykes *et al.* model performs slightly better (Figs. 4 and 5). It should be remembered, however, that the use of the logarithmic profile in the Sykes *et al.* model is justified only when $|z/L_*| < 0.1$. This imposes the condition

$$\frac{h_s}{h} \geqslant \frac{(10k_u)^2}{a_1^3}. \tag{14}$$

Grachev *et al.* (1997) took $a_1 = 2$ (from LESs). Then Eq. (14) became $h_s \geqslant 2h$. With the field-measurement estimate of $a_1 = 5.8$, the above condition, Eq. (14), becomes much less restrictive, namely, $h_s \geqslant 0.08h$. Nevertheless, even in this case the logarithmic profile is impossible throughout unless $z_{0u}/h > 10^{-3}$. However, at such high values of the ratio z_{0u}/h_s, the roughness elements (with typical height $\sim 30z_{0u}$) immediately affect the flow up to heights of order $10^2 z_{0u}$, which gives practically no room for the logarithmic profile. Therefore, in spite of a good correspondence with available data, the Sykes *et al.* model is oversimplified.

In the present paper, stability corrections to the logarithmic profiles in Eq. (6) are introduced using the full Paulson approximation of the functions $\psi_{\{u,T\}}$, namely,

$$\frac{U_*}{W_*} = C_u k_u \left\{ \ln\left(\frac{h}{z_{0u}} \frac{U_*^2}{a_1 W_*^2} \right) - \Psi_u\left(\frac{k_u}{a_1} \frac{W_*}{U_*} \right) + \Psi_u\left(\frac{z_{0u}}{L_*} \right) \right\}^{-1} \tag{15a}$$

$$\frac{Q_s}{\Delta\theta W_*} = -\frac{k_T U_*}{W_*} \left\{ \ln\left(\frac{h}{z_{0T}} \frac{U_*^2}{a_1 W_*^2} \right) - \Psi_T\left(\frac{k_u}{a_1} \frac{W_*}{U_*} \right) + \Psi_T\left(\frac{z_{0T}}{L_*} \right) \right\}^{-1}, \tag{15b}$$

which is valid up to $|z/L_*| \sim 2$. Taking $C_u = 1.55$ and $a = 3.0$, Eq. (15a) agrees with experimental data in Fig. 4 almost perfectly. Here, the ratio $|h_s/L_*|$ is kept lower than 2.0 and the condition $h_s \gg z_{0u}$ is satisfied in the range of $z_{0u}/h < 10^{-4}$. Taking $C_u = 0.8$, Eq. (15a) agrees reasonably well with LES data in Fig. 5.

The Zilitinkevich *et al.* model with an appropriate choice of empirical coefficients fits both experimental and LES data (Figs. 4 and 5). It does not face any physical restrictions at low values of the roughness length. However, its application would not be physically grounded in very strong convection over very rough surfaces, when $30z_{0u} > 0.1L_*$, which gives no room for a logarithmic portion in the wind profile.

In Fig. 6, the dimensionless wind profiles, $u(z)/W_*$, employed in different models are presented in terms of the dimensionless height, z/h, for different values of the dimensionless roughness length, z_{0u}/h. Each profile is plotted up to $z = h_s$, at which height $u(h_s)/W_*$ becomes equal to C_u calculated from field measurements (cf. Eq. (5) and Table 2). In the Zilitinkevich *et al.* model, the wind profile depends on the coefficient $a = h_s/h$. The latter is taken as the same as in the Schumann model, namely, $a = 0.1$. The profiles applied by Zilitinkevich *et al.* and Sykes *et al.* are quite similar, although the surface-layer depth, h_s, in the Zilitinkevich *et al.* model, with $a = 0.1$, is always larger than in the Sykes *et al.* model. Higher up they diverge, since Zilitinkevich *et al.* continues with a different law. Even more similarity is observed between the Zilitinkevich *et al.* model and Eq. (15a) proposed in this paper. With smaller values of a, the dimensionless profiles from the three models, Eqs. (10a), (12a) and (15a), would become almost identical.

The Beljaars model wind profiles are similar to the previous ones at low roughness lengths. At higher roughness, they diverge from the others and do not level off (as already indicated).

The Schumann model diverges from the others at low roughness, showing much lower values of the dimensionless wind speed. As already mentioned, this model is applicable only to convection over quite rough surfaces. For this reason, the Schumann-model wind profiles at z_{0u}/h lower than 10^{-6} are not presented. At higher z_{0u}/h the Schumann-model profiles gradually approach the others.

As clearly seen from the above comparison, the models can be rather successfully fitted to either experimental data or LES data regardless of the underlying physical assumptions. The wind velocity coefficient C_u constitutes the main factor in shifting

the friction velocity curves to fit the chosen data set. The Sykes *et al.* model is the only model that needs two coefficients fitted, C_u and a_1. Empirical values of C_u vary around 1.0 when the curves are adjusted to LES data and around 1.7 when they are adjusted to field measurement.

Higher values for C_u deduced from field measurements could be explained very naturally by spurious contributions from non-zero mean-wind shears to what is supposed to be the minimum friction velocity. Field measurements very rarely represent perfectly calm weather, and some winds (albeit weak) are usually present. In contrast, LES data represent completely shear-free convection.

The convection-induced wind speed approximation, Eq. (5), holds true only in purely shear-free convection. In the presence of a background wind, the squared total wind speed, u_{sca}, becomes

$$u_{\mathrm{sca}}^2 = u_{\mathrm{vec}}^2 + (C_u' W_*)^2, \tag{16}$$

where, u_{vec} is the horizontal vector wind speed and C_u' is a dimensionless parameter (Godfrey and Beljaars 1991).

Equation (16) can be rewritten as $u_{\mathrm{sca}}^2 = u_{\mathrm{vec}}^2 + \alpha'^2(\sigma_u^2 + \sigma_v^2)$, where α' tends to 0.9 for isotropic conditions as u_{vec} vanishes (Jabouille *et al.* 1996; Redelsperger *et al.* 2000) and $\sigma_{\{u,v\}}^2$ are the horizontal velocity variances. In the convective surface layer, the latter are proportional to the Deardorff velocity, W_*. Numerous atmospheric, laboratory and LES data (e.g. Garratt 1992; Hibberd and Sawford 1994; Yaglom 1994) suggest $\sigma_u^2 \approx \sigma_v^2 = (0.4 \pm 0.2) W_*^2$, which gives $C_u' = 0.75 \pm 0.20$.

In the absence of the mean wind ($u_{\mathrm{vec}} = 0$), Eq. (16) reduces to Eq. (5), indicating that C_u' should be equal to C_u when evaluated at h_{s}. Data from the Schmidt and Schumann (1989) and Sykes and Henn (1989) LESs considered in this section satisfy this requirement and suggest $C_u' = C_u \approx 1$.

However, field data from the measurement campaigns TOGA COARE, SCOPE and BOREX-95 chosen by Zilitinkevich *et al.* (1998) for validation of their theoretical model included the cases with the mean wind less than 2 m s^{-1}. In fact, typical values of W_* in these data sets were not higher than 2 m s^{-1}. Therefore it is very probable that the contribution from u_{vec}^2 to the total squared wind speed, u_{sca}^2, given by Eq. (16), was of the same order as the contribution from large convective eddies, $(C_u' W_*)^2$. If so, the discrepancy between the LES and the field-data estimates of U_* is immediately explained as contamination of the field data by a non-zero mean-wind shear. Moreover, one could expect vanishing of the systematic difference between the LESs and the field data provided that the mean-wind effect is excluded.

(*b*) *Heat transfer*

The Zilitinkevich *et al.* (1998) heat transfer formulation, Eq. (12b), as well as data from measurement campaigns SCOPE, TOGA COARE and BOREX-95, is given in terms of the aerodynamic heat transfer coefficient, C_{AH}. All other models and LES data are given in terms of $Q_{\mathrm{s}}/\Delta\theta W_*$. Moreover, in LESs the scalar roughness length, z_{0T}, was taken equal to z_{0u}. For comparison, all models and data are presented below in terms of C_{AH}. Then a uniform representation of the models and data is achieved. The Schumann Eq. (7b) becomes

$$C_{\mathrm{AH}}^{-1} = (4k_u k_T^3)^{-1/3} a_{u1}^2 \frac{W_*}{U_*}, \tag{17}$$

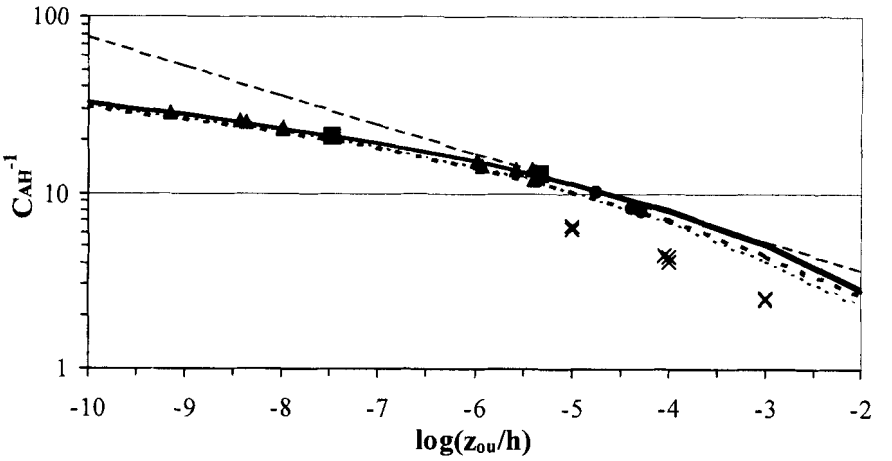

Figure 7. As in Fig. 3, but with all the empirical coefficients in the Schumann (dashed line), Sykes *et al.* (thin line), Beljaars (dotted line), Zilitinkevich *et al.* (heavy line) and Eq. (20) (heavy dotted line) models calculated by fitting to the TOGA COARE (▲), SCOPE (■) and BOREX-95 (•) field data. Large-eddy simulation data (×) are also presented for comparison. The thin line is almost identical to the heavy line.

where the ratio z_{0u}/z_{0T} is not involved.

The Beljaars Eqs. (8a) and (8b) give

$$C_{\mathrm{AH}}^{-1} = C_u k_u k_T^{-1} \frac{W_*}{U_*} + k_T^{-1} \left\{ \Psi_T \left(\frac{z_{0T}}{L_*} \right) - \Psi_u \left(\frac{z_{0u}}{L_*} \right) - \ln \left(\frac{38.5}{4} \right) \right\}, \tag{18}$$

where the terms on the right-hand side, which include z_{0u} and z_{0T}, are negligible.

The Sykes *et al.* Eq. (10b) becomes

$$C_{\mathrm{AH}}^{-1} = C_u a_T k_u \frac{W_*}{U_*} + (a_T - k_T^{-1}) \ln \left(\frac{z_{0u}}{z_{0T}} \right), \tag{19}$$

where the ratio z_{0u}/z_{0T} is present but of secondary importance.

The similar type model with stability corrections, Eq. (15b), becomes

$$C_{\mathrm{AH}}^{-1} = k_T^{-1} \left\{ \ln \left(\frac{h}{z_{0u}} \frac{U_*^2}{a_1 W_*^2} \right) - \Psi_T \left(\frac{k_u}{a_1} \frac{W_*}{U_*} \right) + \Psi_T \left(\frac{z_{0T}}{L_*} \right) \right\}. \tag{20}$$

Theoretical curves representing C_{AH}^{-1} versus $\log(z_{0u}/h)$are shown in Fig. 7 using field data, and in Fig. 8 using LES data. The empirical coefficients involved, both original (when they are known) and newly calculated, are given in Tables 1 and 2. As seen from the figures, field measurements give higher values of C_{AH}^{-1} compared with LESs. In the light of the analysis given in section 3(a), this is immediately explained by the overestimation of U_* in the treatment of field data.

Comparing Figs. 7 and 8, it becomes clear that all models can be adjusted either to LES or to field data through the choice of C_u, keeping all other empirical coefficients unchanged. The only exception is the Sykes *et al.* model. Its adjustment to different data sets involves two coefficients, C_u and a_T, (so that to keep unchanged the ratio a_T/C_u calculated from LESs). The use of recalculated $a_T$values (given in Table 2) almost completely removes the effect of the ratio z_{0u}/z_{0T} on the right-hand side of Eq. (19).

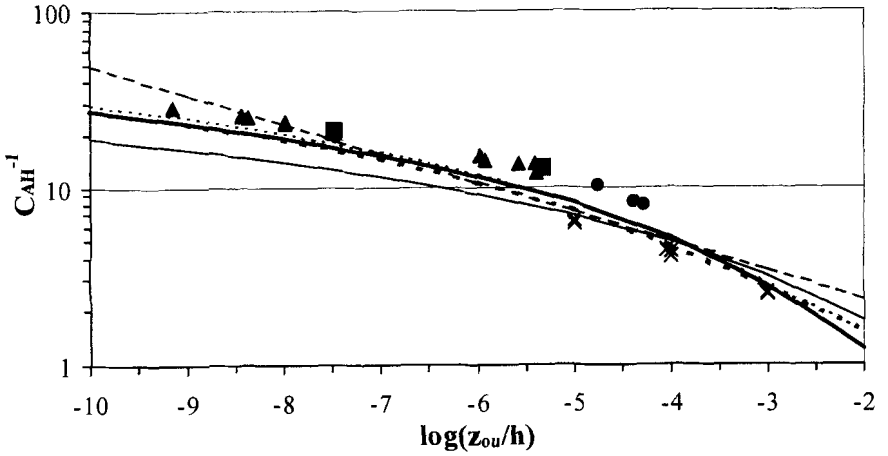

Figure 8. As in Fig. 7, but with all the empirical coefficients in the Schumann (dashed line), Sykes *et al.* (thin line), Beljaars (dotted line), Zilitinkevich *et al.* (heavy line) and Eq. (20) (heavy dotted line) models calculated by fitting to the large-eddy simulation data (×). Field data for TOGA COARE (▲), SCOPE (■) and BOREX-95 (•) are also presented for comparison.

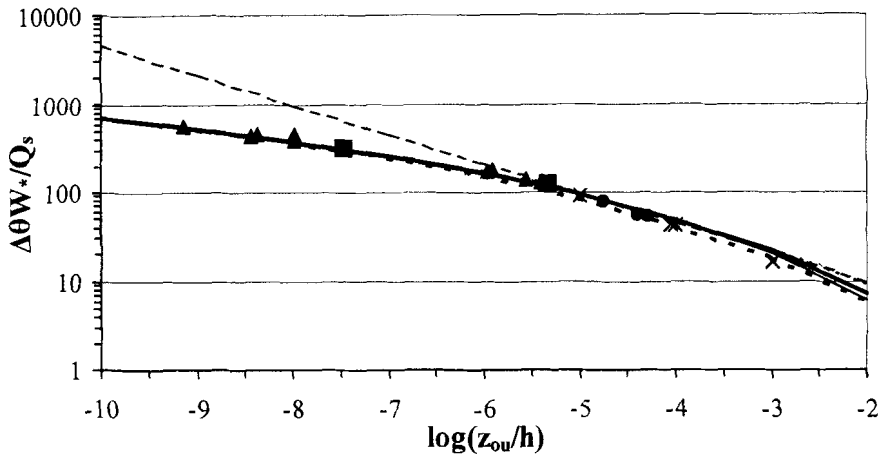

Figure 9. As in Fig. 2, but with all the empirical coefficients in the Schumann (dashed line), Sykes *et al.* (thin line), Beljaars (dotted line), Zilitinkevich *et al.* (heavy line) and Eq. (15b) (heavy dotted line) models calculated from the field data for TOGA COARE (▲), SCOPE (■) and BOREX-95 (•). The roughness lengths, z_{0T} and z_{0u}, were taken as equal. Large-eddy simulation data (×) are also presented for comparison.

In Fig. 7, based on field measurements, theoretical curves are very close to each other and to experimental data over the whole range of z_{0u}/h. The only exception is the Schumann Eq. (17). At small roughness lengths, it strongly overestimates C_{AH}^{-1}. This obviously relates to the underestimation of U_* by the Schumann model already indicated in section 3(a).

In Fig. 8, based on LES data, C_u is taken close to unity. Here, all models show a reasonably good agreement with data. However, LES data cover only a narrow range of z_{0u}/h. Outside this range, the Schumann model and the Sykes *et al.* model diverge, especially at small values of z_{0u}/h.

In Fig. 9, the same type of comparison is presented in terms of the heat transfer coefficient $Q_s/\Delta\theta W_*$, based on the Deardorff velocity-scale W_*. Accordingly, field data are recalculated, and Eq. (12b) is reformulated multiplying it by the ratio W_*/U_*. The curves in Fig. 9 show $\Delta\theta W_*/Q_s$ versus $\log(z_{0u}/h)$. The most important result from this figure is that LES data and field data collapse. Thereafter, it is not surprising that theoretical curves based on the field-data grounded empirical coefficients (taken from Table 2) happened to be in good agreement also with LES data. The only exception is the Schumann model, which essentially diverges from data at low values of z_{0u}/h.

4. Conclusions

The basic results from evaluation of theoretical models of Schumann, Sykes *et al.*, Beljaars, and Zilitinkevich *et al.* are as follows. The Schumann model shows good correspondence with data over quite rough surfaces. The Beljaars model shows good agreement with data on the minimum friction velocity over quite smooth surfaces. The Sykes *et al.*, the Zilitinkevich *et al.*, and the newly proposed Eqs. (15) and (20) models show very similar results. They all perform quite well over the whole range of z_{0u}/h.

Despite differences in the physical assumptions underlying the models, they give similar results and perform quite well when applied either to LESs or to field data. The difference between LESs and field data is more pronounced than the difference between predictions from different models. The key physical problem discussed in this paper is how to explain systematic differences between the LES and the field-data estimates of the minimum friction velocity.

Figures 4, 5 and 9 suggest the following principal conclusion. Even in practically calm weather, the mean-wind shears are pronounced enough to affect empirical estimates of the minimum friction velocity, which causes essential differences between U_*/W_* evaluated from field measurements and LESs. At the same time the heat transfer coefficient $\Delta\theta W_*/Q_s$ is practically insensitive to the above 'calm-weather mean-wind shears', so that the field-measurement and the LES estimates of $\Delta\theta W_*/Q_s$ practically coincide. This fact needs theoretical explanation. At the same time it provides strong argument in support of the LES-grounded estimates of both heat transfer coefficients and minimum friction velocity.

It is shown that adjustment of theoretical curves to the chosen data sets is done mainly through the choice of the 'gustiness coefficient' C_u, Eq. (5). The latter is overestimated using data from field measurements, very probably due to the contribution from uncounted mean-wind shears.

Finally it became clear that LES is an appropriate and efficient technique, which provides high-quality data on the resistance and heat transfer in the convective surface layer.

New analysis of already available and new field data (especially over very rough surfaces) is needed to clarify the role of the mean-wind shear, to validate further the resistance and heat transfer formulations, and to develop a practical flux calculation scheme for use in climate and mesoscale models.

Acknowledgements

This work was supported by the European Union Project SFINCS (Surface Fluxes in Climate System) European Commission Contract ENV4-CT97-0573, and the INTAS Project 96-1692. The authors thank J. C. R. Hunt and A. A. Grachev for helpful discussions.

REFERENCES

Beljaars, A. C. M. 1995 The parametrization of surface fluxes in large scale models under free convection. *Q. J. R. Meteorol. Soc.*, **121,** 255–270

Brutsaert, W. A. 1982 *Evaporation into the atmosphere.* D. Reidel, Dordrecht, the Netherlands

Businger, J. A. 1973 A note on free convection. *Boundary-Layer Meteorol.*, **4,** 323–326

Businger, J. A., Wyngaard, J. C. and Izumi, Y. 1971 Flux profile relationships in the atmospheric surface layer. *J. Atmos. Sci.*, **28,** 181–189

Caughey, S. J. 1982 'Observed characteristics of the atmospheric boundary layer'. Pp. 107–158 in *Atmospheric turbulence and air pollution modelling.* Eds. F. T. M. Nieuwstadt and H. van Dop. D. Reidel, Dordrecht, the Netherlands

Deardorff, J. W. 1970 Convective velocity and temperature scales for the unstable planetary boundary layer. *J. Atmos. Sci.*, **27,** 1211–1213

1972 Parameterization of the planetary boundary layer for use in general circulation models. *Mon. Weather Rev.*, **2,** 93–106

Fairall, C. W., Bradley, E. F., Roger, D. P., Edson, J. B. and Young, G. S. 1996 Air–sea flux parameterization in TOGA COARE. *J. Geophys. Res.*, **101**(C2), 3747–3764

Garratt, J. R. 1992 *The atmospheric boundary layer.* Cambridge University Press

Godfrey, J. S. and Beljaars, A. C. M. 1991 On the turbulent fluxes of buoyancy, heat, and moisture at the air–sea interface at low wind speeds. *J. Geophys. Res.*, **96,** 22043–22048

Grachev, A. A., Fairall, C. W. and Zilitinkevich, S. S. 1997 Surface-layer scaling for the convective induced stress regime. *Boundary-Layer Meteorol.*, **83,** 423–439

Hibberd, M. F. and Sawford, B. L. 1994 A saline laboratory model of the planetary convective boundary layer. *Boundary-Layer Meteorol.*, **67,** 229–250

Jabouille, P., Redelsperger, J. L. and Lafore, J. P. 1996 Modification of surface fluxes by atmospheric convection in the TOGA COARE region. *Mon. Weather Rev.*, **124,** 816–837

Kropfli, R. A. and Clifford, S. F. 1994 The San Clemente Ocean Probing Experiment: A study of air–sea interactions with remote and *in-situ* sensors. IGARSS'94, Pasadena, CA, IEEE, 2407–2409

Mikkelsen, T., Jorgensen, H. E., Lofstrom, P. and Lyck, E. 1996 'Borex-95: Experiment on concentration fluctuations'. Data Report RISØ-R-927(EN)

Monin, A. S. and Yaglom, A. M. 1971 *Statistical fluid mechanics, mechanics of turbulence*, Vol. 1. MIT Press, Cambridge, MA, USA

Paulson, C. A. 1970 The mathematical representation of wind speed and temperature profiles in the unstable atmospheric surface layer. *J. Appl. Meteorol.*, **9,** 857–861

Redelsperger, J. L., Guichard, F. and Mondon, S. 2000 A parameterization of mesoscale enhancement of surface fluxes for large-scale models. *J. Climate*, **13,** 402–421

Schmidt, H. and Schumann, U. 1989 Coherent structure of the convective boundary layer derived from large-eddy simulations. *J. Fluid Mech.*, **200,** 511–562

Schumann, U. 1988 Minimum friction velocity and heat transfer in the rough surface layer of a convective boundary layer. *Boundary-Layer Meteorol.*, **44,** 311–326

Sykes, R. I. and Henn, D. S. 1989 Large-eddy simulation of turbulent sheared convection. *J. Atmos. Sci.*, **46,** 1106–1118

Sykes, R. I., Henn, D. S. and Lewellen, W. S. 1993 Surface-layer description under free-convection conditions. *Q. J. R. Meteorol. Soc.*, **119,** 409–421

Yaglom, A. M. 1994 Fluctuation spectra and variances in convective turbulent boundary layers: a re-evaluation of old models. *Phys. Fluids*, **6,** 962–972

Zilitinkevich, S., Grachev, A. A. and Hunt, J. C. R. 1998 'Surface frictional processes and non-local heat/mass transfer in the shear-free convective boundary layer'. Pp. 83–113 in *Buoyant convection in geophysical flows.* Eds. E. J. Plate *et al.* Kluwer Academic, the Netherlands